Article

Not peer-reviewed version

Biosorption of Manganese Using Moringa oleifera Seed Pods: A Sustainable Approach to Water Treatment

Laura Pinto , Fernanda Tavares , Rosângela Bergamasco , Marcelo Fernandes Vieira , Angelica Vieira *

Posted Date: 1 July 2025

doi: 10.20944/preprints202507.0001.v1

Keywords: Emerging contaminants; heavy metals; Sustainability; waste utilization; Biosorption; Manganese; Chemical modification; oilseed

Preprints.org is a free multidisciplinary platform providing preprint service that is dedicated to making early versions of research outputs permanently available and citable. Preprints posted at Preprints.org appear in Web of Science, Crossref, Google Scholar, Scilit, Europe PMC.

Copyright: This open access article is published under a Creative Commons CC BY 4.0 license, which permit the free download, distribution, and reuse, provided that the author and preprint are cited in any reuse.

Preprints.org (www.preprints.org) | NOT PEER-REVIEWED | Posted: 1 July 2025

doi:10.20944/preprints202507.0001.v1

Disclaimer/Publisher's Note: The statements, opinions, and data contained in all publications are solely those of the individual author(s) and contributor(s) and not of MDPI and/or the editor(s). MDPI and/or the editor(s) disclaim responsibility for any injury to people or property resulting from any ideas, methods, instructions, or products referred to in the content.

Article

Biosorption of Manganese Using Moringa oleifera Seed Pods: A Sustainable Approach to Water Treatment

Laura Adriane de Moraes Pinto [1], Fernanda de Oliveira Tavares [2], Rosangela Bergamasco [2], Marcelo Fernandes Vieira [2] and Angélica Marquetotti Salcedo Vieira [1,*]

[1] Postgraduate Program in Food Science, Universidade Estadual de Maringá, Maringá, PR, Brazil
[2] Postgraduate Program in Chemical Engineering, Universidade Estadual de Maringá, Maringá, PR, Brazil
* Correspondence: amsvieira@uem.br; Tel.: +55 44 3011-5093

Abstract

Manganese can be considered an emerging contaminant, as it is present at levels exceeding those established by authorities in various environments worldwide. Its presence is due to both anthropogenic activities and natural processes. Although it is a natural health promoter, at high levels it can cause damage to humans and the environment. Therefore, this study aimed to utilize the Moringa oleifera seed pod, a byproduct of its production, as a biosorbent for removing Mn from water containing an excess of this ion, thereby contributing to water treatment and reducing environmental liabilities. The biosorbents were prepared from *Moringa oleifera* raw pods and chemically modified using NaOH and HCl, demonstrating their ability to remove Mn(II) from the tested water. EDS, SEM, and FTIR were used to characterize the biosorbents. The experimental data were kinetically analyzed, and it was found that the biosorption of the three different adsorbents followed pseudo-second-order kinetics, with an equilibrium time of 30 minutes. The most efficient biosorbent for manganese removal was the basic-treated pod, achieving a 94% removal rate. The equilibrium data were analyzed using the Langmuir and Freundlich isotherm models, yielding a maximum adsorption capacity of 7.64 mg g^{-1} for the pods with basic treatment and 6.00 mg g^{-1} for the pods in their natural state. The thermodynamic properties were also evaluated, confirming the spontaneous nature of the reaction and the feasibility of the bioremediation process using the pods. The results show that the adopted process is viable, as it removes manganese from contaminated water and provides sustainability for processing waste from *Moringa oleifera* oilseed.

Keywords: emerging contaminants; heavy metals; sustainability; waste utilization; biosorption; manganese; chemical modification; oilseed

1. Introduction

The contamination of aquatic environments represents a critical global concern, contributing substantially to the incidence of various diseases and elevated mortality rates worldwide. Heavy metals, such as manganese (Mn), are frequently detected in industrial effluents, primarily originating from mining, metallurgical processes, and manufacturing activities (Salimi et al., 2025).

Manganese is naturally present in groundwater and, even at low concentrations, can cause several problems in water quality, making its removal essential (Taffarel and Rubio, 2010). Consumption of food and water contaminated with heavy metals is a significant route of human exposure to metals, accounting for approximately 90% of cases. In this regard, the risks associated with metal contamination in foodstuffs have aroused considerable concern worldwide (Khan et al., 2013). Although manganese (Mn) and certain micronutrients are essential for plant growth and human nutrition, they become toxic to the body in high concentrations, as they are not biodegradable and can cause serious adverse effects on human health (Rahman et al., 2012).

© 2025 by the author(s). Distributed under a Creative Commons CC BY license.

Manganese is responsible for some diseases, such as Parkinson's disease, and causes damage to the brain, liver, kidneys, and nervous system; in pregnant women, it affects fetal development and induces abortion, as well as being neurotoxic for children [5, 6].

The presence of manganese in water is a concern for both the population and the industry. High-quality water is of great importance for the production of safe foodstuffs. In the food industry, water is used in all operations, whether directly incorporated into the product as an ingredient or a vehicle for combining ingredients into formulations, or indirectly in processes such as fluid for heat transfer, cleaning and sanitizing equipment, and areas of the process [7]. The presence of manganese in water is directly linked to the oxidation and corrosion of pipes, and it is primarily responsible for imparting an odor, metallic taste, and black discoloration to water distribution and supply systems [8]. Fouling and corrosion in pipes, equipment, and cooling systems increase maintenance costs, reduce operational efficiency, and are a significant source of contamination by manganese [9].

The US Environmental Protection Agency (EPA) sets a maximum level of manganese in drinking water of 0.05 mg L^{-1}. Similarly, the World Health Organization (WHO) has established a limit of 0.1 mg L^{-1}. There is clear evidence of elevated manganese levels in surface waters and effluents, as presented in several works [10, 11, 12, 13]. Therefore, this type of contamination is observed in the most diverse locations around the world, being found in both regions of Brazil, including rivers and industrial effluents, as well as in areas impacted by mining in the Philippines and China.

The survey of metal levels in rivers in the industrial town of Sasolburg revealed higher mean concentrations of Mn, exceeding the guideline limits for domestic and agricultural use set by the WHO and EPA (>50 μg L^{-1}) [12]. High levels of Mn, among other metals, which exceed the maximum permissible concentration limit set by international regulatory organizations, were found by [14] in waters off an island in the Philippines.

Therefore, it is understood that the effective removal of these contaminants from wastewater is crucial for protecting environmental integrity and ensuring the health of ecosystems.

Several physicochemical methods are available for removing heavy metals from aqueous solutions. Among the various water treatment techniques are adsorption, coagulation, advanced oxidation, membrane separation, chemical precipitation, solvent extraction, reverse osmosis, filtration, and electrochemical treatment. Adsorption is preferred for removing heavy metal ions due to its ability to minimize the use of chemicals, ease of handling, variety, and availability of different types of adsorbents, making it a technique considered "eco-friendly" [15,16].

Several alternative processes have been studied to identify economic techniques and low-cost biomaterials for removing heavy metals from water. The biosorption process has some advantages over conventional methods of water purification, such as the replacement of synthetic compounds for natural compounds in the water treatment, low cost, low sludge production, good biodegradability, and is not aggressive to the environment, since most materials used are organic residues [17,18].

Lignocellulosic biomass, primarily composed of cellulose, hemicellulose, and lignin, has garnered attention as a low-cost and sustainable material for water treatment. Its effectiveness as a biosorbent stems from the presence of functional groups on its surface, which can be enhanced through chemical modifications to improve contaminant removal efficiency [19].

Among various plant-based biosorbents, *Moringa oleifera* stands out as the second most studied oilseed species for metal removal, accounting for 32.14% of reported studies [19]. The most commonly used biomass is obtained from the dehulled seed, which, due to its cellulose, hemicellulose, and lignin content, is classified as a lignocellulosic adsorbent [20, 21]. Additionally, according to Meneghel et al. [22], *Moringa oleifera* offers the advantages of anchoring metals, renewability, and low cost, making its use attractive in biosorption processes.

Given the importance of the crops and considering that the processes involved in extracting their oils generate a wide variety of by-products and residues, it is necessary to develop alternatives for the use of these materials, thereby preventing them from becoming an environmental problem. According to Silva et al. [23], the yield of Moringa seed oil can reach 43%. The oil is rich in

© 2025 by the author(s). Distributed under a Creative Commons CC BY license.

monounsaturated fatty acids, primarily oleic acid (~76%), indicating that it is an oilseed with a high-quality fatty acid source and therefore a high capacity for industrial production.

A industrialização cultura da Moringa, hoje em dia, é uma realidade, sendo encontrada em diversas aplicações, incluído produtos de beleza e produção de óleo. No entanto, estudos utilizando os resíduos da produção de Moringa, tal como a casca da vagem, são escassos, o que justifica a pesquisa da sua utilização como biossorvente, de forma a diminuir o impacto ambiental deste resíduo.

Thus, the present study aimed to evaluate *Moringa oleifera* Lam. pods. (Moringa) modified by chemical treatments in Mn biosorption and its removal from aqueous solutions. We studied the influence of parameters such as pH, the adsorbent dose, and the adsorption contact time. Kinetic and equilibrium data, as well as thermodynamic parameters, were obtained.

2. Materials and Methods

All chemical products/reagents used in this study were of analytical grade. A Mn (II) solution (1000 mg. L^{-1}) was prepared, and all other solutions were prepared by diluting this stock solution. A pH meter (Thermo Scientific Orion Versa Star Model) was used to measure the pH. The pH was calibrated with standard buffer solutions of pH 4.0, 7.0, and 9.2. The concentration of Mn (II) metal in the samples was determined after filtering through a cellulose membrane of 0.45mm and quantified in an atomic absorption spectrophotometer (AAS, Varian® AA spectra, 55Australia). The absorbance was measured at a wavelength of 279.5 nm and a spectral bandwidth of 0.2 nm.

2.1. Biosorbents Characterization

The in-natura pod (VAI) and the pretreated pods (VTA and VTB) were characterized before and after the biosorption process by infrared spectroscopy (FT-IR) and scanning electron (SEM). The Scanning electron microscopy with EDS microprobe (SS 550 Superscan Model, Shimadzu®) was used to study the surface morphology of biosorbents and their composition. The FTIR spectrometry analyses were performed using KBr pellets, prepared in a ratio of 1/100 m / m.

The zero charge point (ZCP) was determined for all biosorbents to identify the pH at which the adsorbent surface changes. The methodology used for the determination was proposed by Wang et al. [24], where 0.1 g of adsorbent was added to 50 mL of distilled water at different initial pH conditions, ranging from 1 to 12. The flasks were shaken for 24 hours at 25 °C and 200 rpm. After this period, the samples had their final pH measured and graphically compared with the initial pH values. The acid solutions were adjusted to 0.1 mol. L^{-1} of HCl and the basics with 0.1 mol. $L^{-1}$of NaOH.

2.2. Biomass Modification

Initially, the pods (Figure 1) were separated from the moringa seeds, crushed, washed with distilled water, and dried in a circulating oven at 60 ºC until a constant weight, being called in-natura pods (VAI).

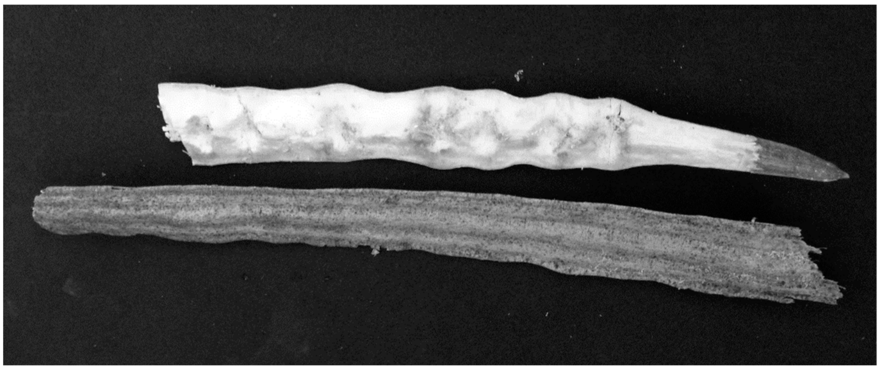

Figure 1. Moringa oleifera pods.

© 2025 by the author(s). Distributed under a Creative Commons CC BY license.

The pod modification was performed using the methodology described by Kumar and Gaur [25], where the evaluated treatment agents were NaOH (0.1 mmol, Synth®, 97% purity) and HCl (0.1 mmol L-1, Synth®, 36.5% purity). These agents were selected due to their known capacity for adsorption improvement [26].

For the basic treatment, VAI was added to the 0.1 mmol NaOH solution in a 3:1 (NaOH volume/moringa mass) proportion, agitated at 80 rpm for 30 minutes at 25 °C. Next, the biomass was centrifuged (300 rpm, 15 min), and the supernatant was discarded. The pellet formed was then washed with Milli-Q water to ensure the removal of excess base. The treated pod was dried in an oven at 60 °C to constant weight. After drying, the material was subjected to particle size patterning with a range of 0.1-0.32 mm, and its manganese removal ability by adsorption was evaluated. This material received the name Basic Treated Pod (VTB). The same procedure was repeated for the treatment agent HCl 0.1 mmol L^{-1}, giving rise to the material named acid-treated pod (VTA)

2.3. Biosorption Experiments

The biosorption experiments were conducted in batch using a sealed plastic flask containing 50 mL of a manganese ion solution at a concentration of 4 mg L^{-1}, with a stirring speed of 200 rpm in a thermostatic bath. The parameters evaluated during the adsorption tests were contact time, pH, temperature, and adsorbent mass, with each parameter varied individually.

The effect of the contact time was evaluated by varying the time from 2 to 150 minutes. A flask containing a Mn ions solution (4 mg L^{-1}) and 0.5 g of biosorbent was stirred at 200 rpm in a thermostated bath at 25 °C for different periods, starting at a pH of 6 (the natural pH of the solution). Finally, the material was filtered through a 0.45 µm cellulose membrane, and aliquots were collected for quantification of metal concentration. A time of 60 min was established as the optimum time for use in subsequent experiments.

The influence of pH was studied by balancing the initial solution (Mn, 4 mg L^{-1}) with NaOH (0.1 mmol) and HCl solution (0.1 mol L^{-1}) for different pH (1.0, 3.0, 5.0, 6.0, 7.0, and 8.0), setting a fixed agitation speed of 200 rpm, adsorbent mass of 0.5 g, a temperature of 25 °C and 60 minutes.

The effect of adsorbent mass was investigated by varying the mass to 0.5, 0.7, 1.0, and 1.3 grams. The experiment was conducted with a Mn(II) concentration of 4 mg L^{-1}, a stirrer speed of 200 rpm, a 60 min contact time, and a temperature of 25 °C, and the optimum pH was determined.

To evaluate the temperature effect, the parameters of metal concentration and rotation were maintained, using 0.5 g of adsorbent mass, an optimal pH found, and temperature varied at 15, 25, 35, and 45 °C with a contact time of 60 min.

After stablishing contact time, metal concentration was measured using AAS. The percentage removal of metal ions was calculated using Eq. (1):

$$Removal\,\% = ((\mathrm{Co} - \mathrm{Cf}) \,/\, \mathrm{Co}) \,.\, 100 \qquad (1)$$

The quantity of metal adsorbed by biomass in equilibrium was calculated using Eq.(2).

$$q = (Co - Ce).V/m \qquad (2)$$

Where Co is the solute concentration in the initial solution (mgL^{-1}); Cf is the final residual metal concentration after the absorption period in mgL^{-1}; Ce is the final solute concentration in equilibrium (mgL^{-1}); V is the solution volume (L), and m is the adsorbent mass (g).

For the study of Mn(II) adsorption isotherms by biosorbents, optimal conditions were applied to each adsorbent, ensuring a balance in the system. The concentration of manganese ions was varied from 5 to 50 mg L^{-1}; the solutions after adsorption were then filtered through a cellulose membrane with a pore size of 0.45 µm, and the metal ions were quantified using an atomic absorption spectrophotometer. In this study, we applied two widely used isotherms, Langmuir and Freundlich, Eqs. (3) and (4) indicate these models respectively.

The Langmuir model [27] used to evaluate the adsorption nature is expressed as:

$$qe = \frac{qmax.KL.Ce}{1+KL.Ce} \qquad (3)$$

© 2025 by the author(s). Distributed under a Creative Commons CC BY license.

In eq. (3) *Ce* (mgL^{-1}) refers to the equilibrium metal concentration, *qe* (mgg^{-1}) is the quantity of metallic ions adsorbed by mass unit of adsorbent in equilibrium state, *qmax* (mgg^{-1}) is the maximum capacity of adsorption, and *KL* (Lmg^{-1}) is the Langmuir constant.

The Freundlich equation can be described as:

$$qe = K_f.Ce^{1/n} \quad (4)$$

Where K_f and *n* are Freundlich constants related to the adsorption capacity and adsorption intensity, respectively, across multiple layers. If the *n*-values were held within 1-10, it indicates that the biosorption process is suitable. For *n* values of 1, the adsorption is linear. Therefore, values lower than *n* indicate that chemical interactions favored adsorption; values greater than *n* characterize the favor of adsorption via physical processes [28].

To evaluate the kinetics of Mn(II) ion removal, pseudo-first-order and pseudo-second-order kinetic models were used to understand the biosorption dynamics of adsorbents VAI, VTA, and VTB.

The pseudo-first-order kinetic model, as proposed by Lagergren [29], is presented below (Eq. 5).

$$Q_t = Q_e(1 - e^{1k_1t}) \quad (5)$$

Where *Qt* (mgg^{-1}) is the quantity of metallic ions adsorbed at moment t, and K1 (min^{-1}) is the pseudo-first order adsorption process constant.

The pseudo-second-order kinetic equation [30] is expressed in Eq. 6.

$$Q_t = \frac{k_2\, Q_e^2 t}{1+k_2 Q_e\, t} \quad (6)$$

Here, Q_e stands for the equilibrium adsorption capacity (mgg^{-1}) and K_2 (gmg^{-1}min^{-1}) is the pseudo-second order adsorption velocity constant.

3. Results Discussion

3.1. Biosorbents Characterization

The characterization of the biosorbent surface and structure is important for understanding the mechanism of interaction between the biomass and the metal [31]. For characterizing and analyzing the composition of surfaces, techniques such as scanning electron microscopy (SEM) with microprobe EDS (Energy Dispersive Spectroscopy) and FTIR analysis were employed.

EDS (Table 1) analysis of the adsorbents (VAI, VTA, and VTB) after Mn(II) adsorption reveals the incorporation of manganese into the samples, as none of the adsorbents initially contained Mn in their composition. The presence of Mn in the samples after the adsorption process confirms the pods ability to adsorb metals. Reddy et al. [32], working with moringa shells, report that compounds present in moringa, such as cellulosic structures and proteins, promote bonding with metals. This is because the metal ion is associated with functional groups present on the biosorbent surface, thereby favoring the biosorption process in moringa.

Table 1. Chemical composition of biosorbents obtained for EDS after adsorption.

	Element (%)					
Biosorbents	C	O	Mg	Al	Ca	Mn
VAI	53.79	45.51	0.14	0.11	0.26	0.19
VTA	53.93	45.11	0.0	0.12	0.29	0.55
VTB	52.00	47.39	0.13	0.12	0.18	0.18

Figure 2 shows the SEM images of the superficial morphology of adsorbents VAI, VTA, and VTB.

© 2025 by the author(s). Distributed under a Creative Commons CC BY license.

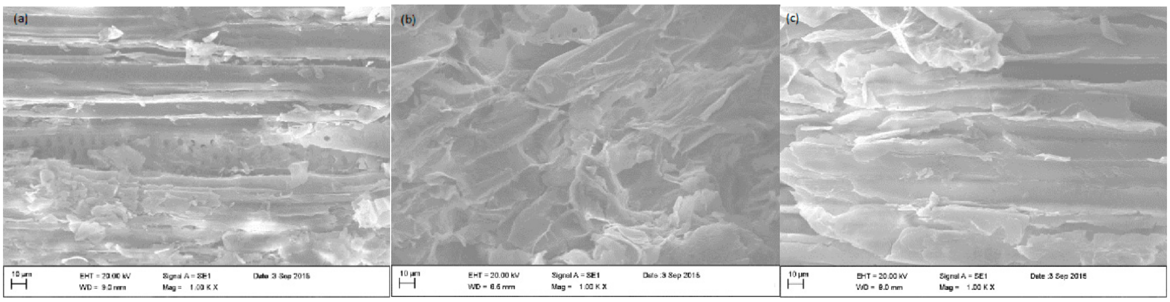

Figure 2. SEM micrographs of adsorbents (A) In-natura pod (VAI), (B) Acid-treated pod (VTA), and (C) Basic-treated pod (VTB).

By analyzing Figure 2, the adsorbents have a surface with a fibrous and heterogeneous appearance, irregular pores of varying dimensions, and are relatively open and asymmetrical. Such features can facilitate the metal biosorption process [22].

FTIR analysis is an effective method for obtaining information about the functional groups present on a material's surface. Figure 3 shows the FTIR spectra of VAI, VTA, and VTB pods.

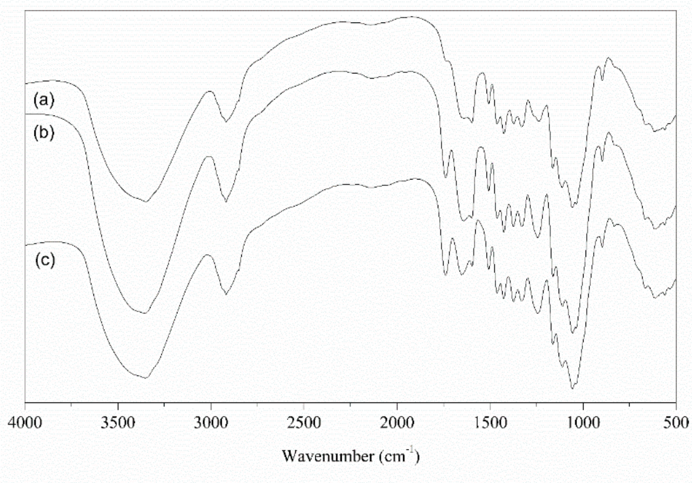

Figure 3. FTIR pods spectrum (A) VTB, (B) VAI, and (C) VTA.

Using FTIR technique, the main functional groups present in the samples were identified. Figure 3 shows a broad band at 3360 cm^{-1}, assigned to the O-H stretching vibration. The peak present at 2923 cm^{-1} is attributed to the symmetric and asymmetric stretch of CH_2; this functional group is present in fatty acids, proteins, cellulose, hemicellulose, and lignin [31]. The peaks in the region of 1740 to 1630 cm^{-1} exhibit a change in intensity, indicating potential changes in the C=O bonds during the proposed treatments. The basic and acid treatments may cause hydrolysis reactions, resulting in the formation of new carboxylic groups (-COO) and hydroxyls (-OH) in the biomass, which can favor metal biosorption [26]. The spectral region of 1224 to 1248 cm^{-1} confirms the presence of carboxylic acids, which is associated with the C-O bond stretching in phenols [22]. The peak at 1054 cm-1 is assigned to C-O type bonds, confirming the presence of a lignin structure that contains functional groups such as hydroxyl and carbonyl, with the capacity to form interactions with metals and remove them. The peak at 893 cm^{-1}is attributed to C-O bonds, characteristic of the presence of cellulosic structures such as hemicellulose and cellulose [33, 34].

Pretreatment promotes the presence of active functional groups such as hydroxyl (-OH) groups and carboxylic groups (-COOH), which are known to promote metal adsorption.

Figure 4 shows the in-natura biomass (VAI) FTIR spectra before and after Mn biosorption. The spectra show an intense band at 3360 cm^{-1}, indicating the presence of hydroxyl groups. The presence of a peak at 2917cm^{-1} can be attributed to the symmetric and asymmetric stretching of the C-H bond. Changing the wave number of the carbonyl band from 1743 cm^{-1} to 1734 cm^{-1} after the adsorption

© 2025 by the author(s). Distributed under a Creative Commons CC BY license.

process indicates the possible connection of metal groups to carboxylic groups. Reddy et al. [32] worked with biomass of *Moringa oleífera* modified leaves as adsorbents for Cd(II), Ni(II) e Cu(II) removal, reporting a similar behavior for their adsorbent, where they claim that such modification is related with the interactions occurred between the carboxylic and hydroxyl groups with metals in solution. From these results, it is assumed that the hydroxyl groups (OH) and carboxyl groups (COOH) preferentially adsorb Mn(II). The subtle shift in the spectra before and after the adsorption process can be associated with the fact that the metal ions concentration is relatively low compared to the adsorbent mass in the adsorption process, which ultimately provides the non-appearance of new peaks and spectrum distortion, characterizing a mild physical adsorption process [26,32]. The pre-treated adsorbents (VTA and VTB) exhibited similar behavior to the in-natura pod in their FTIR spectra, showing a carbonyl band shift at 1743 cm^{-1}, which possibly indicates the formation of metal groups.

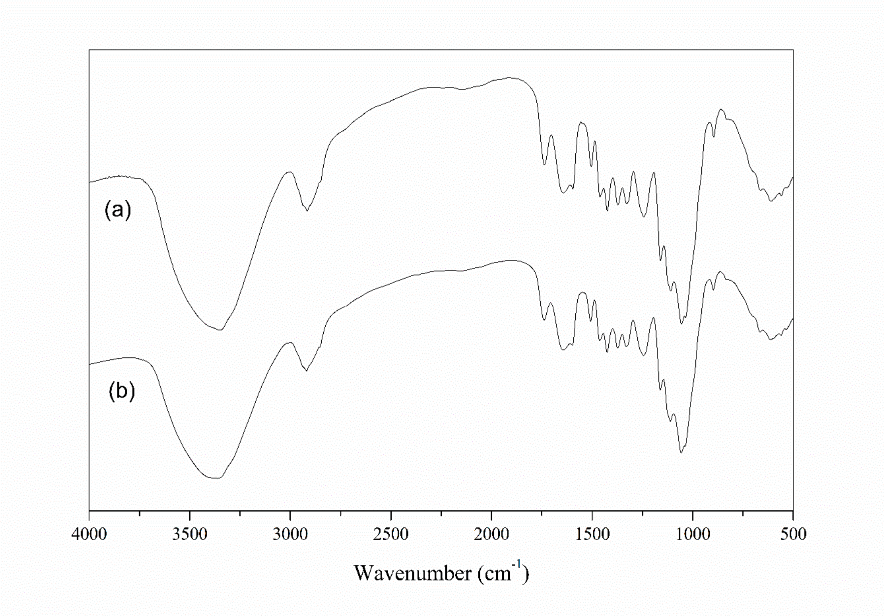

Figure 4. FTIR spectrum of (a) In-natura pod and (b) FTIR spectrum of in-natura pod after manganese adsorption.

Zero Charge Point

Determining the biosorbent zero charge point (ZCP) is crucial for elucidating the biosorption mechanism. Figure 5 shows the ZCP analysis of the studied biosorbents.

Figure 5 illustrates the effect of pH on Mn adsorption for the studied adsorbents. The ZCP values were in the ranges of 6.2-7.2 for VAI, 3.9-4.2 for VTA, and 6.3-8.7 for VTB. This indicates that the biosorbents acquire a positive charge below the ZCP range, and above this value, they acquire a negative charge. At zero charge point, the electrostatic forces between the dissolved Mn (II) ions and the surface of the adsorbent are balanced, so that their charges are canceled. As pH < ZCP, the biosorbent exhibits a positive surface charge, leading to electrostatic repulsion of Mn(II), which reduces its adsorption capacity. When pH > ZCP, the biosorbent surface charges become negative, thereby attracting Mn(II) ions in solution to the surface, which favors adsorption. Reddy et al. [32] reported that metal adsorption is related to both the pH and the nature of the biosorbent, since each biomass has its optimum pH for metal ion adsorption. Thus, different behaviors provide a preliminary indication of the adsorbent's behavior at varying pH levels.

© 2025 by the author(s). Distributed under a Creative Commons CC BY license.

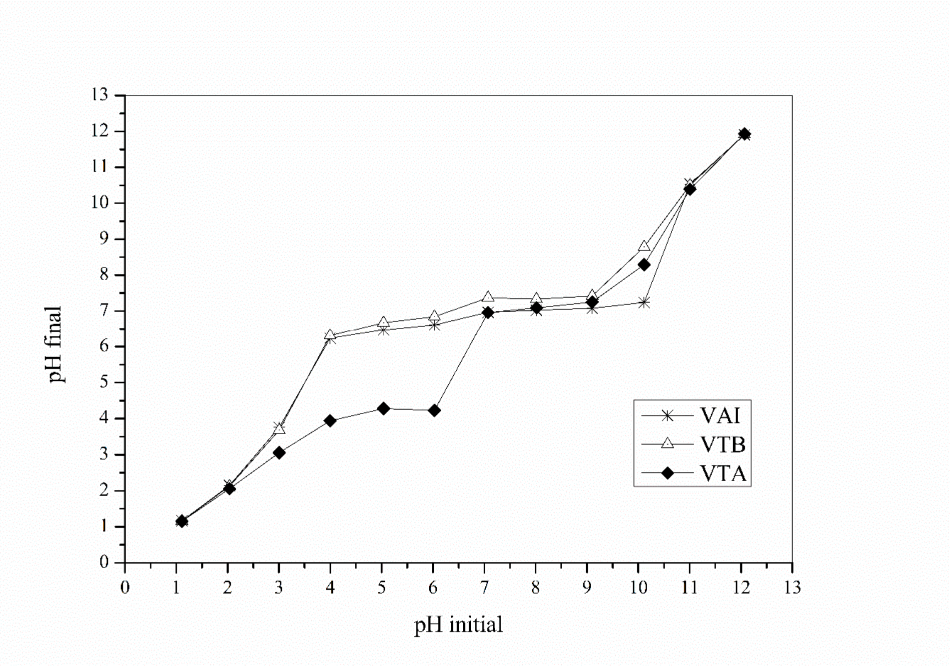

Figure 5. CZP analysis for the VAI, VTA, and VTB biosorbents.

3.2. Contact Time Effect

The effect of contact time on the removal capacity of Mn(II) ions by VAT, VTA, and VTB is shown in Figure 6.

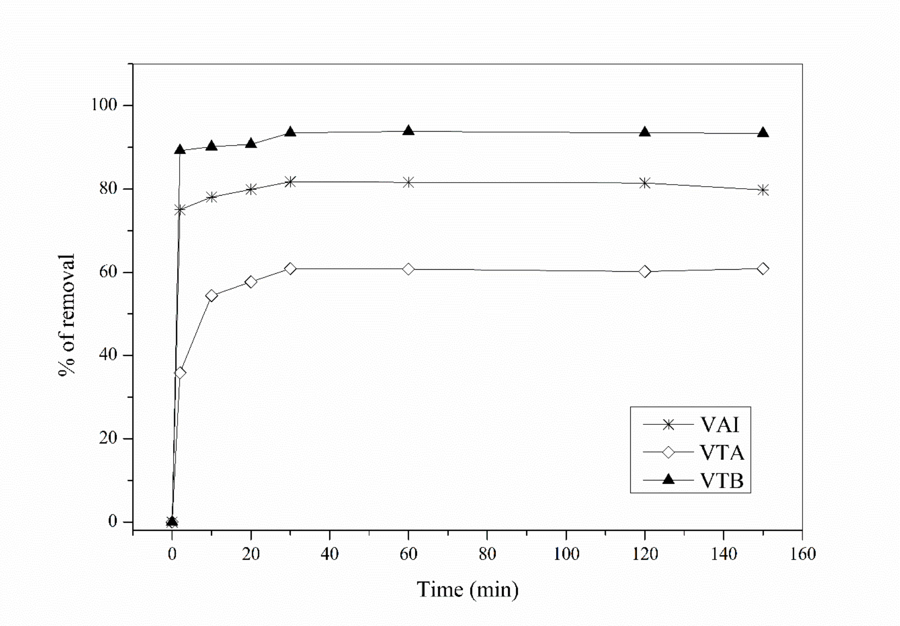

Figure 6. Contact time effect on manganese biosorption of VAI, VTA, and VTB (biosorbent dose: 0.50 g, pH: 6.0).

Analyzing Figure 6, it can be noticed that the adsorption percentage increases with contact time until equilibrium is reached. The contact time study for the three adsorbents (VAI, VTA, and VTB) in the removal of Mn(II) ions from the solution showed that they exhibit similar adsorptive behavior, with most of the metal ions being removed within the range of 2-30 minutes. As shown, the removal percentage increases significantly in the initial phase (0-20 minutes), reaching equilibrium within approximately 30 minutes. The equilibrium between the solution and the adsorbent was reached at 30 minutes for the three adsorbents studied; however, a longer time was chosen to obtain the adsorption isotherm (60 minutes), ensuring the system had reached equilibrium. The maximum

© 2025 by the author(s). Distributed under a Creative Commons CC BY license.

biosorption was 81.70% for VAI, 60.97% for VTA, and 93.85% for VTB, indicating residual manganese in solution of 0.732 mg L^{-1} for the in-natura pod, 1.561 mg L^{-1} for the acid-treated pod, and 0.246 mg L^{-1} for the basic pod. After the treatment, the biomass undergoes a series of changes, including the removal of surface impurities, membrane rupture, and the exposure of new functional groups, such as hydroxyls and carboxylic groups, which may favor or hinder the biosorption process [26].

3.3. pH Influence in the Adsorption Process

The effect of pH on manganese adsorption by the adsorbents VAI, VTA, and VTB, varying the pH from 1 to 8, is shown in Figure 7.

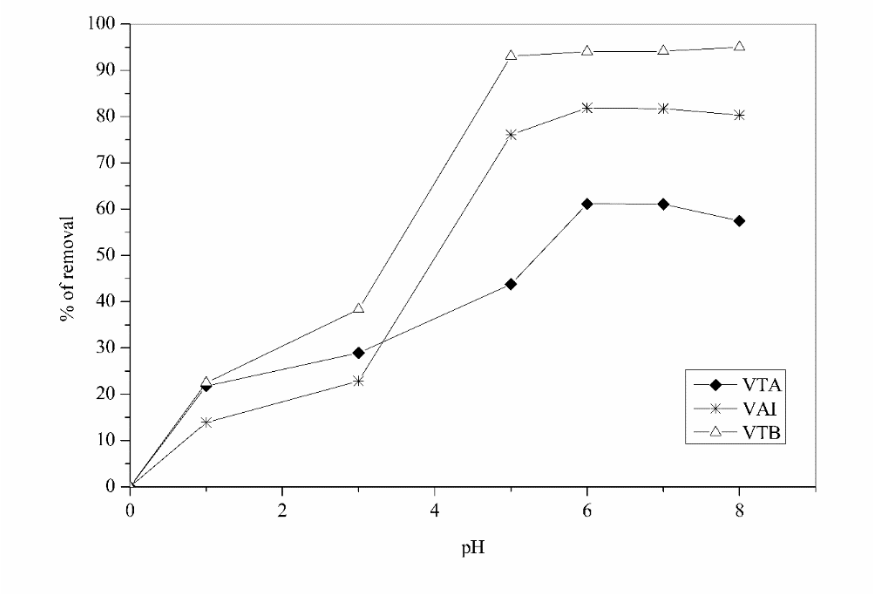

Figure 7. pH effect on Mn biosorption of VAI, VTA, and VTB.

In the adsorption process, the pH of the solution is an important variable, since it directly affects the metals' adsorption due to protonation/deprotonation of functional groups of the adsorbent [15].

It is worth noting that the removal capacity for acid-treated pods (VTA), in-natura pods (VAI), and basic-treated pods (VTB) initially increased with the pH and then remained broadly unchanged from pH 6.0 onwards. The maximum removal was observed in the pH 6-8 range for the three adsorbents studied; therefore, the pH chosen for further studies was six, as this value showed good removal for all adsorbents and is the natural pH of the solution. A study conducted in 2025 for Cardoso et al [35] investigated the potential of coconut shell powder derived from Cocos nucifera agricultural waste as a sustainable biosorbent for removing Mn (II). The study found that the maximum removal efficiency of Mn(II) was 86.4% at pH 7.

At pH levels above 8.0, Mn(II) precipitates as Mn $(OH)_2$, making it unavailable for adsorption; additionally, metal precipitation causes turbidity [22]. The VTA adsorbent's performance in removing Mn (II) ions from solution confirms the data obtained in CZP analysis, where manganese adsorption is favored at higher pH values. As for VAI and VTB, removal was favored in the zero-load range. Variations in metal sorption at different pH levels can be related to the ionic strength [25]. Furthermore, the alkaline treatment can contribute to the exposure of specific chemical groups by reinforcing the connection between the cation and the metal adsorbent [26]. Another factor to correlate is that on the CZP, the adsorbent surface charge tends to be neutral, electrostatic forces between metal ions and the adsorbent surface equilibrate, and even in equilibrium, certain carboxylic and hydroxyl groups present in the sorbent molecule are further available for connecting with metals (Kalavathy & Miranda, 2010).

3.4. Biosorbent Dose Effect

© 2025 by the author(s). Distributed under a Creative Commons CC BY license.

Preprints.org (www.preprints.org) | NOT PEER-REVIEWED | Posted: 1 July 2025 doi:10.20944/preprints202507.0001.v1

The Mn (II) biosorption by the studied adsorbents (VAI, VTA, and VTB) was evaluated by varying the adsorbent amount from 0.5 to 1.5 g in solution, with an initial concentration of 4 mg L^{-1}, pH 6, and a contact time of 60 minutes. The effect of the biosorbent dose on Mn (II) adsorption is shown in Figure 8.

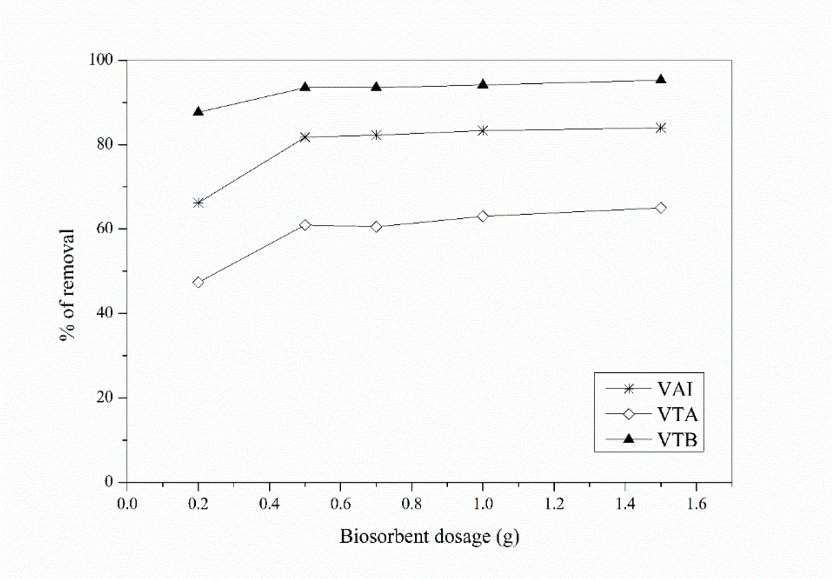

Figure 8. Biosorption dose effect in Mn (II) adsorption of VAI, VTA, and VTB.

The in-natura pod demonstrated a satisfactory removal capacity; therefore, for the pre-treatments, the alkaline treatment showed better removal than the acid treatment. The removal percentage varied from 66% to 83% with the in-natura pod, from 47% to 65% with the acid-treated pod, and from 87% to 95% with the basic-treated pod. Obtaining a residual manganese in solution of 0.68 mg L^{-1}, 1.4 mg L^{-1}, and 0.2 mg L^{-1}, respectively, for the VTI, VTA, and VTB pods. As the adsorbent dose was increased, the adsorbent's efficiency also rose; however, it remained constant starting from the 0.5 g dose, which justified the use of a 0.5 g biosorbent mass for further studies. This result can be explained by the fact that increasing the amount of biomass, the surface area, and the number of active sites available for new connections increases, improving the bioremediation capacity [17]. Furthermore, Lalhruaitluanga et al. [28] reported that alkali biomass pretreatments improve the adsorption capacity compared to untreated biomass, as they may contribute to the availability of specific functional groups responsible for anchoring metals, thereby enhancing the biomass's adsorption capacity.

3.5. Temperature Effect in Biosorption

With a contact time of 60 min, pH 6, and a fixed adsorbent dose of 0.5 g, the effect of temperature on the adsorption of Mn ions per VAI, VTA, and VTB was studied at temperatures ranging from 15 to 45 °C. The effect of temperature variation is shown in Figure 9.

Figure 9 displays the Mn removal capacity of VAI, VTA, and VTB adsorbents as a function of temperature variation. The removal ranged from 79% to 85% for VAI, 61% to 62% for VTA, and 92% to 94% for VTB, resulting in residual manganese solutions of 0.6 mgL^{-1} for the in-natura pods, 1.52 mgL^{-1} for the acid-treated pods, and 0.24 mgL^{-1} for the basic-treated pods.

© 2025 by the author(s). Distributed under a Creative Commons CC BY license.

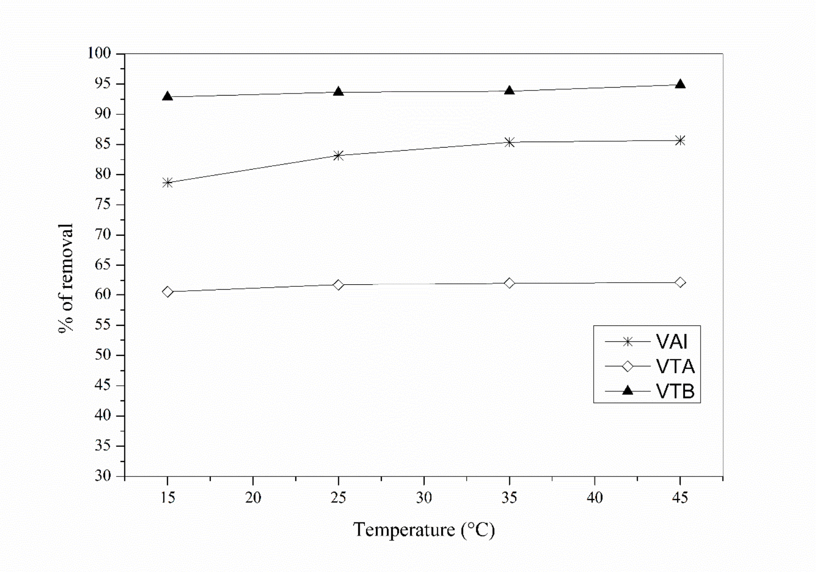

Figure 9. Temperature effect on Mn removal capacity of VAI, VTA and VTB.

The results show that for all three adsorbents, biosorption is enhanced with increasing temperature. This fact is due to the endothermic nature of the adsorption process, whereas as the temperature rises, adsorption tends to increase. However, the temperature variation showed no significant difference in manganese biosorption capacity at 25 °C, which was chosen as the temperature for further studies. Tounsadi and colleagues [16], when working with Diplotaxisharra and Glebioniscoronaria L. biomass for Cd (II) and Co (II) adsorption, observed that the temperature did not influence their adsorptive process. This fact is associated with the morphological nature of the biosorbent, which lacks defined pores, thereby not favoring the adsorption process.

3.6. Kinetic Study

The kinetic parameters of the adsorbents studied are shown in Table 2.

Table 2. Kinetic parameters of biosorbents VAI, VTA, and VTB onto the Mn(II) adsorption process.

Biosorbents	Q_{eexp} (mg g^{-1})	Pseudo-first-order		
		$Q_{t\ cal}$ (mg g^{-1})	K_1 (min^{-1})	R^2
VAI	0.34	0.32±0.00	1.40±0.09	0.998
VTA	0.24	0.24±0.01	0.37±0.04	0.979
VTB	0.37	0.37±0.00	1.75±0.08	0.999
		Pseudo- second-order		
		$Q_{t\ cal}$ (mg g^{-1})	K_2(g mg^{-1}min^{-1})	R^2
VAI		0.32±0.00	19.56±1.10	0.999
VTA		0.25±0.00	2.33±0.19	0.996
VTB		0.37±0.00	36.45±1.25	0.999

C_o = 4.0 mg L^{-1}; T=25 °C.

As shown in Table 2, both models fit the kinetic data. However, the pseudo-second-order model is the one that best describes the biosorption of Mn (II) by moringa pods, presenting the most significant R^2 coefficient values (0.996-0.999) and values closer to Q_{eexp} and Q_{tcal}, reinforcing the applicability of this model. The second-order kinetic model suggests that the limiting rate stage was adsorption, indicating that the adsorption process is dependent on the amount of adsorbed metal on the adsorbent surface and the amount adsorbed at equilibrium [36].

© 2025 by the author(s). Distributed under a Creative Commons CC BY license.

3.7. Equilibrium Isotherms

The experimental data fitted to the Langmuir and Freundlich experimental models are shown in Figure 10.

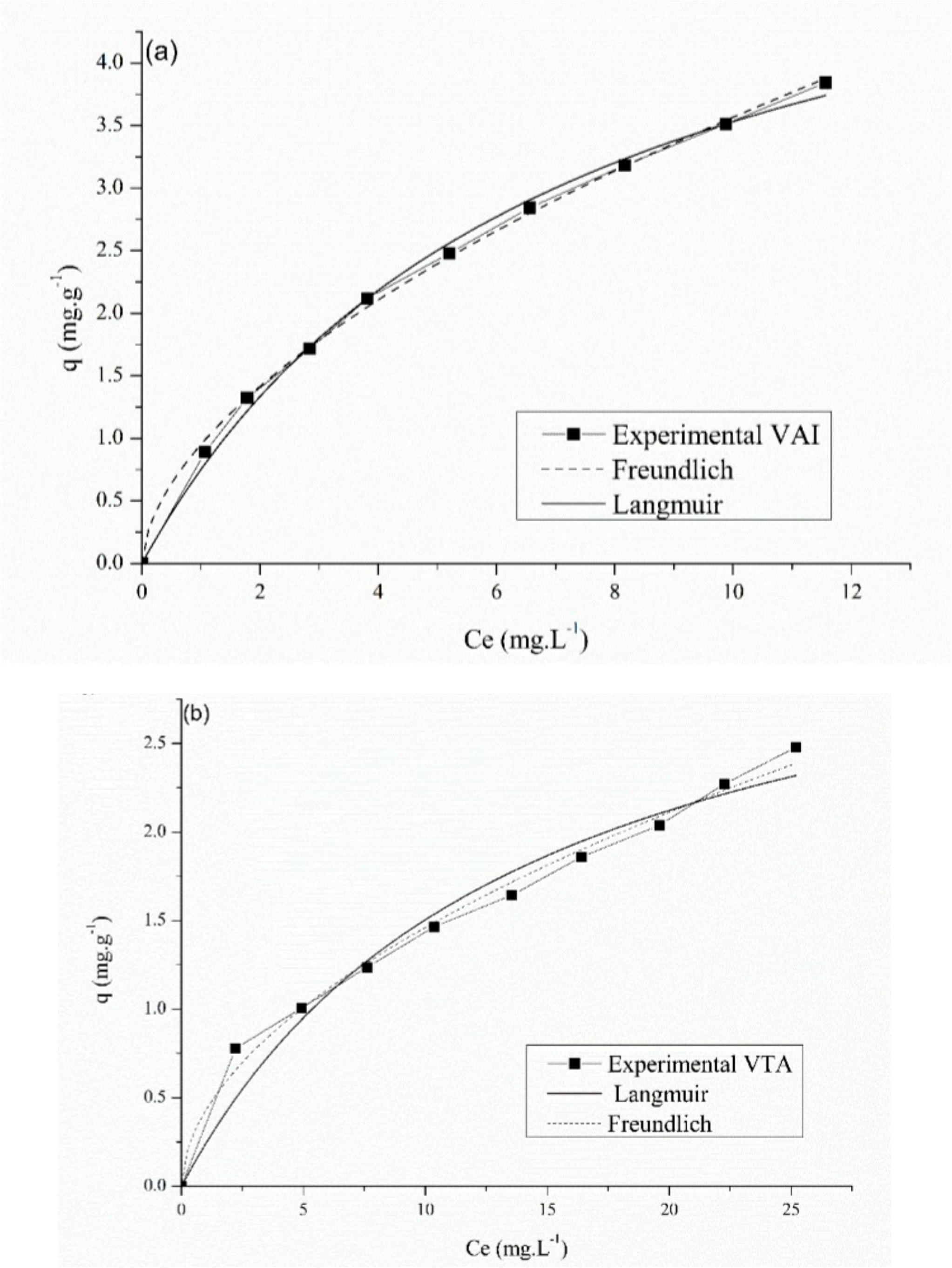

© 2025 by the author(s). Distributed under a Creative Commons CC BY license.

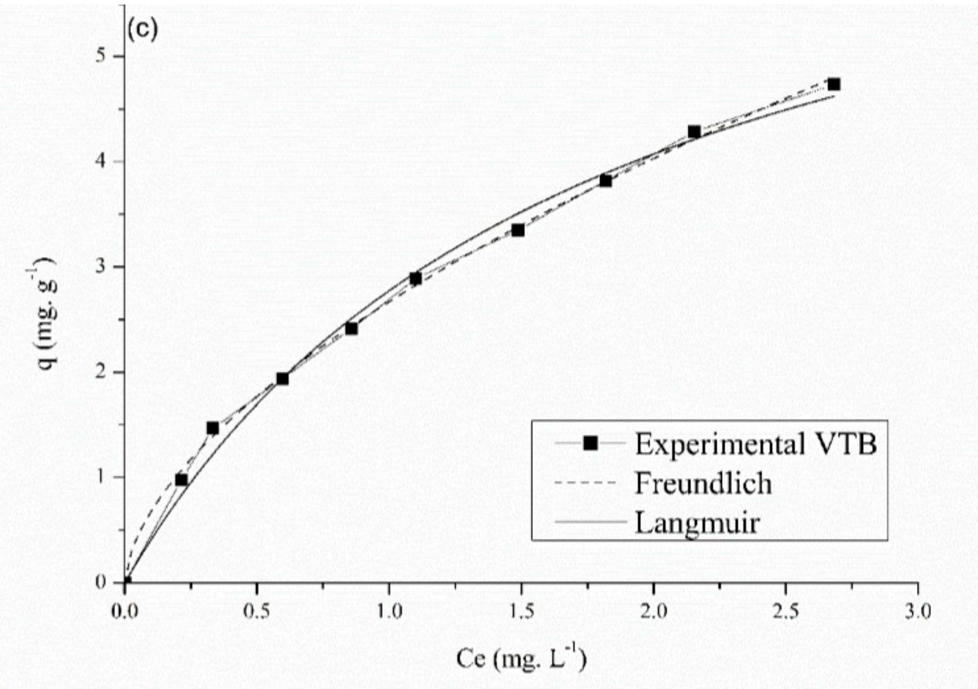

Figure 10. Langmuir and Freundlich isotherms adjusted to manganese adsorption experimental data at 10 to 50 mg L^{-1}, 50 mL volume, 0.5 g of adsorbent at 25°C, pH 6, and time of 60min for VAI (a), VTA (b), and VTB (c) adsorbents.

The adsorption isotherm expresses the relation between the biosorbent amount per gram of adsorbed metal ions, in addition to providing information on the adsorption behavior [17]. Several isothermal models have been widely used to determine a model for the system equilibrium adsorption. The most commonly used models are the Langmuir and the Freundlich, where the Langmuir adsorption model assumes that it occurs over a homogeneous monolayer surface without any interaction between the adsorbed ions.

On the other hand, the Freundlich equation is an empirical model based on adsorption onto a heterogeneous surface, implying that adsorption occurs in multiple layers, where the energy diminishes exponentially with increasing surface coverage. The parameters obtained for each model are given in Table 3.

Table 3. Isotherm parameters for Mn (II).

Biosorbents	Langmuir			Freundlich		
	q_{max} (mg g^{-1})	KL (L mg $^{-1}$)	R^2	Kf (mg$^{1-1/n}$ L$^{1/n}$ g^{-1})	n	R^2
VAI	6.00±0.25	0.14±0.01	0.99	0.95±0.02	1.74±0.04	0.99
VTA	3.60±0.42	0.07±0.02	0.97	0.43±0.32	1.88±0.94	0.99
VTB	7.64±0.50	0.57±0.07	0.99	1.68±0.04	2.67±0.02	0.99

As shown in Table 3, the experimental data for VAI, VTA, and VTB biosorbents were well-fitted by the Langmuir and Freundlich models, with higher R^2 values, indicating that the calculated biosorption capacity using these models is close to the experimental values obtained. The Freundlich isotherm confirms the heterogeneity of the adsorbent surface sites, as the values of n are between 1 and 10, indicating that the biosorption of Mn ions for the studied adsorbents was favorable. It was also observed that the maximum adsorption capacity (q_{max}) was 7.64 mg g^{-1} for VTB, 6.00 mg g^{-1} for VAI, and 3.60 mg $g^{-1}$for VTA.

© 2025 by the author(s). Distributed under a Creative Commons CC BY license.

3.8. Biosorption Thermodynamics

The temperature effect on the adsorption of Mn (II) ions by the adsorbent was studied at 15, 25, 35, and 45°C, with a constant concentration of 4 mg L^{-1}, pH 6.0, and a contact time of 60 min. The dependence of the equilibrium constant (Kc) for the Mn ions adsorption was calculated for all temperatures using Eq. (7):

$$Kc = \frac{Fe}{1-Fe} \quad (7)$$

Where, Fe is the percentage sorption fraction in equilibrium. The thermodynamic parameters, Gibbs free energy ($\Delta G°$), enthalpy variation ($\Delta H°$) and entropy variation ($\Delta S°$) [37] were calculated using equations (8) and (9):

$$ln\,Kc = -\frac{\Delta H}{R.T} + \frac{\Delta S}{R} \quad (8)$$

$$\Delta G° = -R.T.ln\,Kc \quad (9)$$

Here, R is the universal gas constant (8.314 J(mol K)$^{-1}$) and T is the absolute temperature (K). The values of ΔH° and ΔS° can be calculated using the intersection of ln Kc vs 1 / T rect. The thermodynamic parameters for the adsorption process using different biosorbents are presented in Table 4.

Table 4. Thermodynamic parameters used in Mn (II) adsorption for the different adsorbents used.

Biosorbent	**−ΔG°**(KJ. mol^{-1})				**ΔH°** (KJ.mol^{-1})	**ΔS°** (J. mol $^{-1}$.K^{-1})
	288 K	298 K	308 K	318 K		
VAI	9.34	12.18	14.85	15.71	11.88	52.10
VTA	1.08	1.18	1.25	1.30	1.08	7.49
VTB	6.12	6.64	6.95	7.67	8.94	51.61

The negative ΔG° values obtained at different temperatures for all adsorbents confirm the spontaneous nature of the reaction, as well as the viability of the biosorption process. For ΔH° values found for all samples were positive, confirming the endothermic nature of the process. The positive entropy value indicates the system's tendency towards randomness during the adsorption process [17].

4. Conclusion

This study revealed that the basic treatment showed a maximum biosorption capacity of 7.64 mg g-1 for the pods with basic treatment, and 6.00 mg g-1 for the pods in their natural state. The optimal adsorption condition achieved a residual manganese content of 0.24 mg L^{-1} in the treated water, an acceptable value according to the EPA. Furthermore, the pseudo-second-order model provides the best fit for the kinetic data. The results demonstrate that the biosorption process using *Moringa oleifera* pods, particularly those subjected to basic treatment, is an efficient and feasible method for removing manganese from contaminated water. The pseudo-second-order kinetics, high adsorption capacity, and spontaneous nature of the reaction confirm the potential of this technique as a sustainable alternative for bioremediation and the valorization of agro-industrial waste. Additionally, these biosorbents are renewable and biodegradable.

Acknowledgments: The authors would like to thank the government agencies National Council for Scientific and Technological Development (CNPq) and Coordination for the Improvement of Higher Education Personnel (CAPES), financial code 001, for their financial support of the research.

References

Abdeen, Z., Mohammad, S.G., Mahmoud, M.S. Adsorption of Mn (II) ion on polyvinyl alcohol/chitosan dry blending from aqueous solution. Environ. Nanotechnol. Monit. Manag. 2015, 3, 1–9.

© 2025 by the author(s). Distributed under a Creative Commons CC BY license.

Preprints.org (www.preprints.org) | NOT PEER-REVIEWED | Posted: 1 July 2025 doi:10.20944/preprints202507.0001.v1

Agarin, C. J. M.; Mascareñas, D. R.; Nolos, R.; Chan, E.; Senoro, D. B. Transition Metals in Freshwater Crustaceans, Tilapia, and Inland Water: Hazardous to the Population of the Small Island Province. Toxics 2021, 9, 71.

Akhtar, M., Moosa Hasany, S., Bhanger, M.I., Iqbal, S. Sorption potential of Moringa oleifera pods for the removal of organic pollutants from aqueous solutions. J. Hazard. Mater. 2007, 141, 546–556.

Alfarra, S.R., Ali, E.N. and Yusoff, M.M. Removal of Heavy Metals by Natural Adsorbent. Int. J. Bios., 2014, 4, 130-139.

Alves, V.N., Coelho, N.M.M. Selective extraction and preconcentration of chromium using Moringa oleifera husks as biosorbent and flame atomic absorption spectrometry. Microchem. J. 2013, 109, 16–22.

Anastopoulos, I., Kyzas, G.Z. Progress in batch biosorption of heavy metals onto algae. J. Mol. Liq. 2015, 209, 77–86.

Araújo, C. S. T.; Carvalho, D. C.; Rezende, H. C.; Almeida, I. L. S.; Coelho, L. M.; Coelho, N. M. M.; Marques, T. L.; Alves, V. N. Bioremediation of Waters Contaminated with Heavy Metals Using Moringa oleifera Seeds as Biosorbent. Patil, Y. (Ed.). (2013). Applied Bioremediation - Active and Passive Approaches. InTech. doi: 10.5772/50859

Cardoso, A. P.; Valdiviezo-Gonzales, N. S. C. L.; Veneu, D. M.; Pino, A. H.; Torem, M. L. Comparative evaluation of lead and manganese removal from contaminated water using cocos nucifera shell powder in batch and continuous adsorption systems. S. Afr. J. Chem. Eng. 2025, 53, 483–494.

Esfandiar, N., Nasernejad, B., Ebadi, T. Removal of Mn(II) from groundwater by sugarcane bagasse and activated carbon (a comparative study): Application of response surface methodology (RSM). J. Ind. Eng. Chem. 2014, 20, 3726–3736.

Hermes, N.; Schneider, R. C. S.; Molin, D. D.; Riegel, G. Z.; Costa, A. B.; Corbellini, V. A.; Torres, J. O. M.; Malm, O. Environmental pathways and human exposure to manganese in southern Brazil. An. Acad. Bras. Ciênc. 2013, 85 (4).

Ho, Y. S. and Mckay, G. The kinetics of sorption of basic dyes from aqueous solution by sphagnum moss peat. The Canadian Journal of Chemical Engineering, 1998, 76, 822-827.

Hoyland, V.W., Knocke, W.R., Falkinham, J.O., Pruden, A., Singh, G. Effect of drinking water treatment process parameters on biological removal of manganese from surface water. Water Res. 2014, 66, 31–39.

Kalavathy, H. and Miranda, M. L.R. Moringa oleifera-A solid phase extractant for the removal of copper, nickel and zinc from aqueous solutions. Chem. Eng. J. 2010, 158, 188–199.

Kasaai, M.R. Use of Water Properties in Food Technology: A Global View. Int. J. Food Prop. 2014, 17, 1034–1054.

Khan, M.U., Malik, R.N., Muhammad, S. Human health risk from Heavy metal via food crops consumption with wastewater irrigation practices in Pakistan. Chemosphere, 2013, 93, 2230–2238.

Kumar, D., Gaur, J.P. Metal biosorption by two cyanobacterial mats in relation to pH, biomass concentration, pretreatment and reuse. Bioresour. Technol. 2011, 102, 2529–2535.

Lagergren, S. Zur theorie der sogenannten adsorption gelster stoffe, Kungliga Svenska Vetenskapsakademiens. Handlingar, 1898, 24, p. 1-39.

Lalhruaitluanga, H., Jayaram, K., Prasad, M.N. V, Kumar, K.K. Lead(II) adsorption from aqueous solutions by raw and activated charcoals of Melocanna baccifera Roxburgh (bamboo)-A comparative study. J. Hazard. Mater. 2010, 175, 311–318.

Langmuir, I. The adsorption of gases on plane surfaces of glass, mica and platinum. J. Am. Chem. Soc. 1918, 40, 1361–1403.

Marques, T.L., Alves, V.N., Coelho, L.M., Coelho, N.M.M. Removal of Ni(II) from aqueous solution using Moringa oleifera seeds as a bioadsorbent. Water Sci. Technol. 2012, 65, 1435–1440.

Melo, D. F. B. C.; Ribeiro, M. H. G.; Albuquerque Junior, E. C.; Gonçalves, E. A. P. Avaliação da Bacia do Rio Una-Pernambuco: Perspectiva da Qualidade da Água após a Construção de 4 Barragens para Contenção de Cheias Revista Brasileira de Geografia Física, 2018, 11, 612-627.

Meneghel, A.P., Gonçalves, A.C., Rubio, F., Dragunski, D.C., Lindino, C.A., Strey, L. Biosorption of cadmium from water using moringa (Moringa oleifera Lam.) Seeds. Water. Air. Soil Pollut. 2013, 224, 1–13.

Mollo, V. M.; Nomngongo, P. N.; Ramontja, J. Evaluation of Surface Water Quality Using Various Indices for Heavy Metals in Sasolburg, South Africa. Water, 2022, 14, 2375.

© 2025 by the author(s). Distributed under a Creative Commons CC BY license.

Preprints.org (www.preprints.org) | NOT PEER-REVIEWED | Posted: 1 July 2025 doi:10.20944/preprints202507.0001.v1

Monjardin, C. E., Power, C., & Senoro, D. B. Spatio-Temporal Assessment of Manganese Contamination in Relation to River Morphology: A Study of the Boac and Mogpog Rivers in Marinduque, Philippines. Sustainability, 2023, 15, 8276.

Nwagbara, V. U.; Iyama, W. A.; Chigayo, K.; Kwaambwa, H. M. Efficiency of *Moringa Oleifera* Seed Biomass in the Removal of Lead (II) Ion in Aqueous Solution. Eur. J. Appl. Sci, 2022, 10, 2.

Pena-Guzman, C.; Otalvaro-Alvarez, A.; Jimenez-Ariza, T. Use of oilseed crops biomass for heavy metal treatment in water. Oil Crop Science 9, 2024, 177–186.

Peng, C.-Y., Korshin, G. V., Valentine, R.L., Hill, A.S., Friedman, M.J., Reiber, S.H. Characterization of elemental and structural composition of corrosion scales and deposits formed in drinking water distribution systems. Water Res. 2010, 44, 4570–4580.

Rahman, M.M., Dong, Z., Naidu, R. Concentrations of arsenic and other elements in groundwater of Bangladesh and West Bengal, India: Potential cancer risk. Chemosphere, 2015, 139, 54–64.

Rahman, M.S., Molla, A.H., Saha, N., Rahman, A.. Study on heavy metals levels and its risk assessment in some edible fishes from Bangshi River, Savar, Dhaka, Bangladesh. Food Chem. 2012, 134, 1847–1854.

Reddy, D.H.K., Seshaiah, K., Reddy, a. V.R., Lee, S.M. Optimization of Cd(II), Cu(II) and Ni(II) biosorption by chemically modified Moringa oleifera leaves powder. Carbohydr. Polym. 2012, 88, 1077–1086.

Salimi, A.; Ghanbarizadeh, P.; Mirvakili, A.; Moheimani, N. R. Optimizing heavy metal remediation of synthetic wastewater using Chlorella vulgaris and Sargassum angustifolium: A comparative analysis of biosorption and bioaccumulation techniques. STOTEN, 2025, 992, 179938.

Silva, M. O.; Camacho, F. P.; Ferreira-Pinto, L.; Giufrida, W. M.; Vieira, A. M. S.; Visentainer, J. V.; Vedoy, D. R. L.; Cardozo-Filho, L. Extraction and Phase Behaviour of *Moringa oleifera* Seed Oil Using Compressed Propane. Can. J. Chem. Eng. 2016, 94, 2195-2201.

Taffarel, S.R., Rubio, J. Removal of Mn2+ from aqueous solution by manganese oxide coated zeolite. Miner. Eng. 2010, 23, 1131–1138.

Tounsadi, H., Khalidi, A., Abdennouri, M., Barka, N. Biosorption potential of Diplotaxis harra and Glebionis coronaria L. biomasses for the removal of Cd(II) and Co(II) from aqueous solutions. J. Environ. Chem. Eng. 2015, 3, 822-830.

Usepa, 2004. Drinking Water Health Advisory for Manganese, in: U.S. Environmental Protection Agency Office of WaterWashington, DC EPA-822-R-04-003. pp. 1–49. doi:EPA-822-R-04-003.

Wang, L., Zhang, J., Wang, A. Removal of methylene blue from aqueous solution using chitosan-g-poly(acrylic acid)/montmorillonite superadsorbent nanocomposite. Colloids Surfaces A Physicochem. Eng. Asp. 2008, 322, 47–53.

Zafar, M.N., Aslam, I., Nadeem, R., Munir, S., Rana, U.A., Khan, S.U.-D. Characterization of chemically modified biosorbents from rice bran for biosorption of Ni(II). J. Taiwan Inst. Chem. Eng. 2015, 46, 82–88.

Disclaimer/Publisher's Note: The statements, opinions and data contained in all publications are solely those of the individual author(s) and contributor(s) and not of MDPI and/or the editor(s). MDPI and/or the editor(s) disclaim responsibility for any injury to people or property resulting from any ideas, methods, instructions or products referred to in the content.

© 2025 by the author(s). Distributed under a Creative Commons CC BY license.